

# Field-Simulation-Based Strategy for Designing Microstrip Filters

Elena Semouchkina<sup>1</sup>, George Semouchkin<sup>1</sup>, Michael Lanagan<sup>1</sup>, and Raj Mittra<sup>2</sup>

<sup>1</sup>Materials Research Institute, <sup>2</sup>Department of Electrical Engineering, The Pennsylvania State University, University Park, Pennsylvania 16802, USA

**Abstract** — Insertion loss spectrum of microstrip open-loop square ring band-pass filter is analyzed by using the Finite Difference Time Domain (FDTD) field simulations. Visualization of standing waves at resonant frequencies guides the placement of stepped impedance sections or capacitive loads at electric field maxima. Strategic load placement enables us to modify selected resonant modes, to monitor efficiently center and attenuation pole frequencies, to affect the shape and width of the pass-band, and to alter the input impedance. The presented approach is useful for miniaturizing various types of microstrip filters and antennas and optimizing their performance.

## I. INTRODUCTION

Recently there has been a growing interest in the application of microstrip band-pass filters in the next-generation wireless and mobile communication systems. These filters have low profile and are able to provide space, weight and cost savings. In addition, microstrip filters with elliptical function response are notable due to narrow band and low insertion loss.

Canonical elliptical filters built with open-loop square rings have been described by Hong and Lancaster [1], however, they are relatively large in size. It is possible to reduce the size by introducing stepped impedance or capacitive load in the device design. Stepped impedance has been frequently used in resonators, including microstrip ones [2]. Capacitive loadings of different types have been often introduced in monopole and patch antennas to reduce their dimensions [3, 4]. In a more recent paper, Hong and Lancaster used stepped impedance principle and proposed the use of open-loop filters having the microstrip width, gradually increasing toward the slot, which resulted in reduced size and wider upper stop-band of the filter [5]. Further size reduction and improvement of the characteristics of an open-loop filter was reported by Banciu *et al.* [6], who introduced symmetrically located stepped impedance parts and open stubs in each ring section of the filter.

In this paper we develop a strategy for the placement either the capacitive loads or stepped impedance sections in open-loop microstrip filters based on the results of simulation field distribution at resonant frequencies. This

enables us to selectively modify the resonant modes and to monitor pass-band characteristics of the filter.

## II. RESULTS AND DISCUSSION

### A. Analysis of $S_{21}$ Spectrum Using Field Simulation

Fig. 1 shows the geometry and the insertion loss spectrum of one section of microstrip open-loop square ring filter. A microstrip section above the loop was added to model the coupling with the next section, and to calculate the  $S_{21}$  spectrum. The substrate was 0.66 mm thick and had a dielectric constant of 9; the width of microstrips was 1 mm.

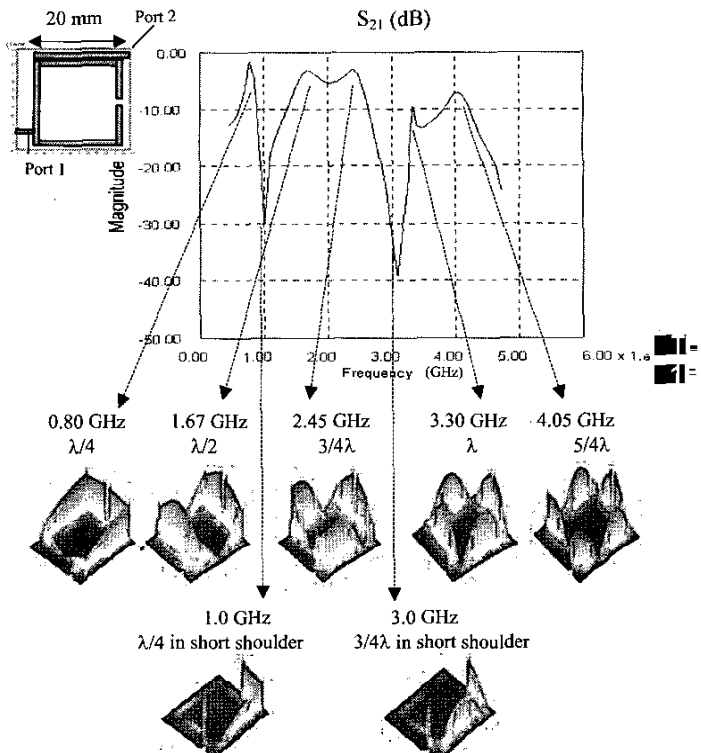


Fig. 1. A single section of open-loop square ring filter,  $S_{21}$  spectrum, and standing wave patterns corresponding to the peaks and attenuation poles of the spectrum.

Simulations were performed by using the FDTD method. A Gaussian-shaped electric field pulse, modulated by a sine wave, was applied between the microstrip and the ground plane to excite the structure. Time domain simulation results were converted into the frequency domain data using the Fast Fourier Transformation, which allowed visualization of the field standing wave patterns at the resonant frequencies [7]. The FDTD method has the advantage of accounting for geometrical details of the structure, as well as for the type and location of the feed that is important for correct identification of the resonant modes excited in the structure.

An open-loop square ring resonator is known to support the  $\lambda/4$  mode resonance, which can provide efficient coupling of multiple sections in canonical band-pass filters [1]. However, the pass-band of the  $\lambda/4$  mode is not accompanied by a lower frequency attenuation pole. This is clearly seen from Fig. 1, which presents the simulated  $S_{21}$  spectrum of an open-loop square ring filter and standing wave patterns of the normal electric field component at the frequencies corresponding to the peaks and attenuation poles of the spectrum. The first peak observed at the frequency 0.8 GHz corresponds to the  $\lambda/4$  resonance; the second one at 1.67 GHz is related to the  $\lambda/2$  mode and it partly overlaps with the third peak at 2.45 GHz, which corresponds to the  $3/4\lambda$  mode. The composite band for these two modes is accompanied by two attenuation poles that could be used for defining the pass-band in the single-section filter. Therefore, we have studied the effects of stepped impedance and capacitive loading on the performance of the filter in this band. We also took into account the next two partially superimposed peaks at 3.3 GHz and 4.05 GHz that corresponded to the  $\lambda$  and  $5/4\lambda$  modes, respectively.

The data presented in Fig. 1 also serve to explain how the attenuation poles in the  $S_{21}$  spectrum are formed. The first pole, at 1 GHz, corresponds to the  $\lambda/4$  resonance in the right shoulder (the shorter one) of the square ring between the input feedline and the gap, while the second pole at 3 GHz is associated with the  $3/4\lambda$  resonance in the same shoulder. Both these resonances provide zero field in the left shoulder (the longer one) of the ring and, therefore, we observe zero signal in the output feedline and attenuation poles in the  $S_{21}$  spectrum.

#### B. Resonant Mode Modification Using Stepped Impedance or Capacitive Loading

As shown in Fig. 1, the filter characteristics are influenced by seven resonant modes that have different standing wave patterns. At resonance, the areas of maximum field in the structure correspond to capacitive type of electrical performance. Therefore, if we place

capacitive loads or stepped impedance sections, which serve to introduce additional capacitances, at the locations of field maxima of the resonant mode, this will effectively change the resonant frequency of this mode, but would not affect the modes that have zero electric fields at the same locations. The use of such an approach opens the possibility of selectively affecting the resonant modes. The data presented below illustrate the effects of patch-type stepped impedance sections placed at different areas of the open-loop filter.

Fig. 2 shows the schematics of geometry and simulation results for open-loop resonators with stepped impedance sections located near the slot (column-a) and in the middle of the front rib (column-b).

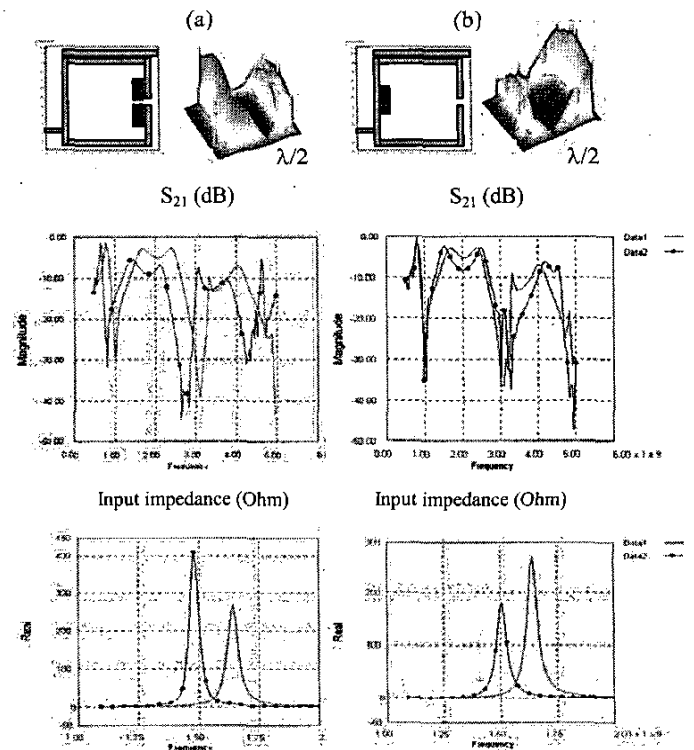


Fig. 2. (a) Geometries, field patterns for  $\lambda/2$  mode,  $S_{21}$  and input impedance spectra for filters with stepped impedances located: (a) near the slot and (b) in the middle of the front rib. Data1-filter without load, Data2-filters with stepped impedances.

For both types of stepped impedance loadings depicted in Fig. 2, the  $\lambda/2$  mode of the filter is modified in similar manner, *viz.*, its wavelength increases while its resonant frequency goes down. The same effect occurs for all the other modes depicted in Fig. 1, when the load is located near the ring slot, since all the modes have field maxima at this location. This results in a shifting of the entire  $S_{21}$

spectrum to lower frequencies, as seen from the  $S_{21}$  plot in Fig. 2 (column-a). When the load is located in the middle of front rib, it affects the modes  $\lambda/2$ , and  $\lambda$  in a similar way, but does not alter the modes  $\lambda/4$ ,  $3/4\lambda$  and  $5/4\lambda$ , since they have zero fields at this location. The corresponding peaks in the  $S_{21}$  spectrum do not shift, as is evident from Fig. 2, column-b.

The input impedance of the filter increases for the first type of loading, while its behavior is opposite for the second type. The results demonstrate that it is possible to change the resonant frequencies of the selected modes and to match the input impedance of the filter by changing the locations of the stepped impedances.

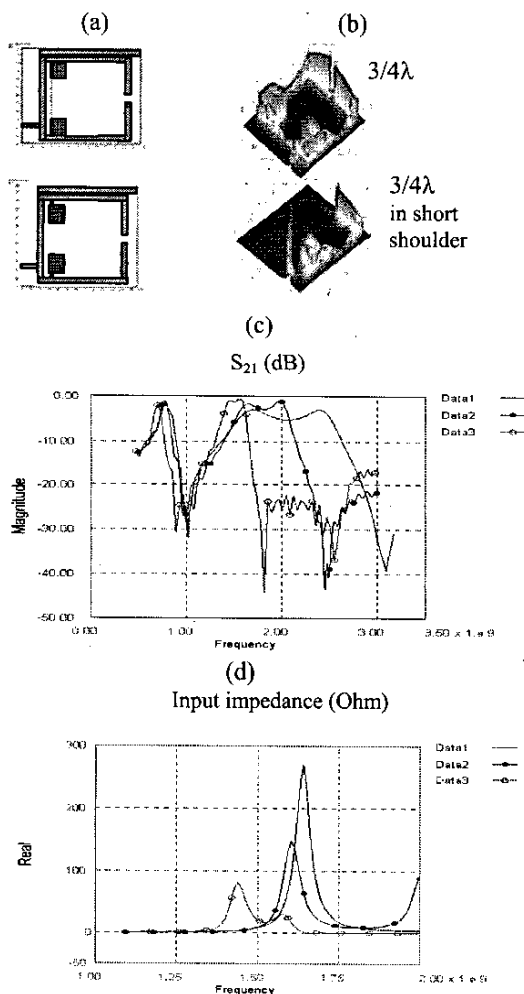


Fig. 3. (a) Geometries of stepped impedance and capacitive loading, (b) field patterns of  $3/4\lambda$  mode and  $3/4\lambda$  in right shoulder, (c)  $S_{21}$ , and (d) input impedance spectra: Data1-unloaded filter, Data2-filter with stepped impedance, and Data3-filter with capacitive loading.

Fig. 3-illustrates the effects of stepped impedance and capacitive loading at the locations of field maximums for the  $3/4\lambda$  mode of the filter. Fig. 3a shows the geometries of the filter with patch-type stepped impedance sections and of the one with patch sections separated from the side ribs by a 0.8 mm gap, and connected with them by 0.4 mm wide microstrips. The latter design allows us to provide a capacitive loading of the filter precisely at the desired points.

Fig. 3b depicts the standing wave patterns of the modified  $3/4\lambda$  mode and of the mode responsible for the second attenuation pole of the filter. The modes  $\lambda/4$  and  $\lambda/2$  are expected to be less affected by the loading at the side ribs than the  $3/4\lambda$  mode, since they do not have maximum field at these locations (see field patterns in Fig. 1). This is confirmed by the results of simulation  $S_{21}$  spectra in the loaded structures (Fig. 3c), which show a strong shift of the  $3/4\lambda$  peak, as well as of the second attenuation pole, to lower frequencies and a very slight shift of the  $\lambda/4$  and  $\lambda/2$  peaks.

Fig. 3c also demonstrates that capacitive loading of the filter at discrete points, where the  $3/4\lambda$  resonant mode has electric field maximums, is more effective in modifying the resonant frequency and input impedance, than adding distributed stepped impedance sections at the same locations (see Figs. 3c and 3d).

Fig. 3c also shows that a selective shifting of the  $3/4\lambda$  mode that does not change the  $\lambda/2$  mode, enables us to realize a narrow pass-band with two attenuation poles for a single section open-loop filter, which is typically used as a  $\lambda/4$  mode filter and provides one attenuation pole in the insertion loss spectrum.

Table I summarizes the data on the effect of the patch-type stepped impedances, placed at four different locations, on the resonant frequencies of the different modes and on the input impedance of the filter. The locations of loading are schematically shown in the left column. The arrows pointing up or down indicate increase or decrease of the resonant frequency or of the impedance. The three different arrow lengths depict the magnitude of the frequency change.

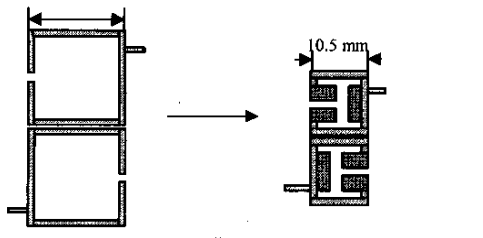
It is worth to note that the effect of stepped impedance (or capacitive load) increases with increase of the area of stepped impedance section. A combination of different sized patch sections placed at different locations can provide the desired filter size and characteristics.

Fig. 4 demonstrates a possibility of miniaturizing a two-section open-loop square filter by using patch-type loads placed at different locations. As seen for the figure, the area of the filter loaded with three additional patches is twice less than one of the unloaded filter, while the  $\lambda/2$  band is observed at the same frequency of 2.45 GHz.

TABLE I  
EFFECT OF LOAD LOCATION ON RESONANT FREQUENCIES OF  
DIFFERENT MODES AND INPUT IMPEDANCE

Load location	Resonant frequency $\lambda/4$	Resonant frequency $\lambda/2$	Resonant frequency $3/4\lambda$	Resonant frequency $\lambda$	Input impedance
	↓	↓	↓	↓	↑
	No effect	↓	No effect	↓	↓
	↓	↓	↓	↓	↓
	↓	No effect	No effect	↓	↓

(a)



(b)

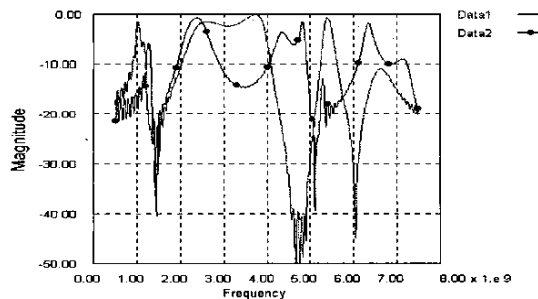


Fig. 4. (a) Geometries of an unloaded two-section filter and of a filter with stepped impedance sections located: two near the slit, area of each patch- $15 \text{ mm}^2$  and one in the middle of the front rib, area of the patch- $12 \text{ mm}^2$ ; and (b)  $S_{21}$  spectra: Data1-unloaded filter, Data2-filter loaded with three patches.

### III. CONCLUSION

We have shown, *via* the example of a microstrip open-loop square ring band-pass filter, how the field analysis of the resonant modes can be applied for strategic placement of the stepped impedance sections or capacitive loads. The possibility to selectively affect the resonant modes and to change center and attenuation pole frequencies, shape and width of the pass-band and of the upper stop band, as well as to match input impedance is demonstrated. We have shown how to realize a narrow pass-band with two attenuation poles in single section open-loop filter and to reduce the device size. We have also found that the capacitive loading of the filter exactly at the points, where the resonant mode has electric field maxima, is more efficient than introducing stepped impedance sections at the same locations.

The developed approach can be used to optimize the design and to miniaturize microstrip filters and antennas. It is especially useful for device geometries that support complex standing wave patterns and multiple resonances.

### ACKNOWLEDGEMENT

This work was supported by the National Science Foundation, as part of the Center for Dielectric Studies under Grant No. 0120812.

### REFERENCES

- [1] J.S.Hong, and M.J.Lancaster, "Canonical microstrip filter using square open-loop resonator," *Electron. Lett.*, vol 31, pp. 2020-2022, 1995.
- [2] M.Sagawa, M.Makimoto, and S.Yamashita, "Geometrical structures and fundamental characteristics of microwave stepped-impedance resonators," *IEEE Trans. Microwave Theory Tech.*, vol. 45, pp.1078-1085, 1997.
- [3] D.Lacey, G.Drossos, Z.Wu, L.E.Davis, T.W.Button, and P.Smith, "Miniaturized HTS microstrip patch antenna with enhanced capacitive loading," *IEE, Savoy Place, London WC2R 0BL*, pp.4/1-4/6, 1996.
- [4] C.Delaveaud, P.Leveque, and B.Jecko, "Small-sized low-profile antenna to replace monopole antennas," *Electron. Lett.*, vol. 34, pp. 716-717, 1998.
- [5] J.S.Hong, and M.J.Lancaster, "Theory and experiment of novel microstrip slow-wave open-loop resonator filters", *IEEE Trans. Microwave Theory Tech.*, vol. 45, pp. 2358-2365, 1997.
- [6] M.G.Banciu, R.Ramer, and A.Ioachim, "Microstrip filters using new compact resonators," *Electron. Lett.*, vol. 38, pp. 228-229, 2002.
- [7] E. Semouchkina, W. Cao, R. Mittra, and W. Yu, "Analysis of resonance processes in microstrip ring resonators by the FDTD method," *Microwave Optical Tech. Lett.*, vol. 28, pp. 312-321, 2001.